UNIL | Université de Lausanne
Faculté de biologie
et de médecine

Mémoire de Maîtrise en médecine

Neuronal responses in mouse barrel cortex:
Comparison of two signal discriminators

Etudiant
Killian Scartezzini

Tuteur
Prof. Egbert Welker

Expert
Dr. Ron Stoop

DBCM - Département de Biologie Cellulaire et de Morphologie, Lausanne, 2011

Abstract

Barrels are discrete cytoarchitectonic neurons cluster located in the layer IV of the somatosensory cortex in mice brain. Each barrel is related to a specific whisker located on the mouse snout. The whisker-to-barrel pathway is a part of the somatosensory system that is intensively used to explore sensory activation induced plasticity in the cerebral cortex.
Different recording methods exist to explore the cortical response induced by whisker deflection in the cortex of anesthetized mice. In this work, we used a method called the *Single-Unit Analysis* by which we recorded the extracellular electric signals of a single barrel neuron using a microelectrode. After recording the signal was processed by discriminators to isolate specific neuronal shape (action potentials).
The objective of this thesis was to familiarize with the barrel cortex recording during whisker deflection and its theoretical background and to compare two different ways of discriminating and sorting cortical signal, the *Waveform Window Discriminator* (*WWD*) or the *Spike Shape Discriminator* (*SSD*).
WWD is an electric module allowing the selection of specific electric signal shape. A trigger and a window potential level are set manually. During measurements, every time the electric signal passes through the two levels a dot is generated on time line. It was the method used in previous extracellular recording study in the *Département de Biologie Cellulaire et de Morphologie* (*DBCM*) in Lausanne.
SSD is a function provided by the signal analysis software *Spike2* (*Cambridge Electronic Design*). The neuronal signal is discriminated by a complex algorithm allowing the creation of specific templates. Each of these templates is supposed to correspond to a cell response profile. The templates are saved as a number of points (62 in this study) and are set for each new cortical location. During measurements, every time the cortical recorded signal corresponds to a defined number of templates points (60% in this study) a dot is generated on time line. The advantage of the *SSD* is that multiple templates can be used during a single stimulation, allowing a simultaneous recording of multiple signals.
It exists different ways to represent data after discrimination and sorting. The most commonly used in the *Single-Unit Analysis* of the barrel cortex are the representation of the time between stimulation and the first cell response (the latency), the representation of the *Response Magnitude* (*RM*) after whisker deflection corrected for spontaneous activity and the representation of the time distribution of neuronal spikes on time axis after whisker stimulation (*Peri-Stimulus Time Histogram, PSTH*).
The results show that the *RMs* and the latencies in layer IV were significantly different between the *WWD* and the *SSD* discriminated signal. The temporal distribution of the latencies shows that the different values were included between 6 and 60ms with no peak value for *SSD* while the *WWD* data were all gathered around a peak of 11ms (corresponding to previous studies). The scattered distribution of the latencies recorded with the *SSD* did not correspond to a cell response.
The *SSD* appears to be a powerful tool for signal sorting but we do not succeed to use it for the *Single-Unit Analysis* extracellular recordings. Further recordings with different *SSD* templates settings and larger sample size may help to show the utility of this tool in *Single-Unit Analysis* studies.

Key words

Barrel, Cortex, Somatosensory, Electrophysiology, Sorting

Mémoire de Maîtrise en médecine

Neuronal responses in mouse barrel cortex:
Comparison of two signal discriminators

Introduction

1. Abbreviations

ATP	Adénosine Triphosphate
EEG	Electroencephalogram
LFP	Local Field Potential
SmI	Primary Sensory Cortex;
VB	Ventrobasal Nucleus of the thalamus
POm	Medial Division of the Posterior Nucleus of the thalamus
PMBSF	Posteromedial Barrel Subfield Region
PW	Principal Whisker
CRF	Center Receptive Field
SW	Surrounding Whiskers
SRF	Surround Receptive Field
RM	Response Magnitude
PSTH	Peri-Stimulus Time Histogram
PIR	Postinhibitory Rebound
TC	Thalamo-Cortical
SD	Standard Deviation
CSD	Current Source Density
SUA	Single-Unit Analysis
MUA	Multi-Unit Activity
WWD	Waveform Window Discriminator
SSD	Spike Shape Discriminator

Theory

2. What is electrophysiology?

The etymology of electrophysiology is issued from the melting of to specific words. The word *electric*, which first use goes back to the XVIIth century when the English scientist William Gilbert used it to describe the attraction force deployed by rubbed amber (*êlektron* in ancient Greek). Physiology, as for it, takes its origin into two Greek words *phusis*, the nature, the way of being and *logos* the speech, the story. We now enter in the study of the electrochemical phenomenons, which occur into cells or living organisms.

The history of this knowledge goes back to the Ancient Time, but in the 18th century only did this field distinguish itself from classical Physiology thanks to the work of Luigi Galvani. He observed in 1791, while he was dissecting a frog, that the contact between its scalpel and the sciatic nerves of the animal was inducing muscular contraction: he named this phenomenon *animal electricity*. From this work hundred of theories took birth to conduce to our actual vision of cellular conduction.

The cellular membrane is an electric insulating layer placed between two aqueous conducting substrates. The presence of multiple ion channels permits to maintain a negative polarity inside the cell compared to its external environment. This creates a difference of potential called the *electric potential of the cell membrane*. The ion channels (especially Na/K channels) contribute to the maintenance of the membrane potential by pumping ions through the cell membrane against their gradients. This mechanism required a huge amount of energy that is extracted from the molecule of *ATP*. Some specific body cells, called *excitable cells* (neurons and muscular cells) have the capacity, when a certain threshold is reached, to change this electric potential very quickly through a phenomenon called *depolarization*. This *depolarization*, based on specific ion channel openings, (principally Na^+ channels in neurons) is followed by a *repolarization* (K^+ channels) frequently accompanied by a hyperpolarisation state. These two consecutive phenomenons are called an *Action Potential* (*Figure 1*).

In order to explore the electric activity in the brain, the first methodical tool used in the pioneering works of neurophysiology was the recording of mass action potentials, i.e. the electroencephalogram (*EEG*). Despite its easy application, the major problem of this technique is that the signal resulting from multiple action potentials coming from multiple cells is measured and is issued from different unknown brain depth and cortical regions. It therefore presents a very poor spatial resolution (Mitzdorf, 1985).

Specific electrophysiological techniques allow measuring the variation of a single cell membrane potential, such as the *patch clamp*, an intracellular way of recording. This device offers an incredible sensitivity and time resolution to potential cell variations, but requires a specific control of the membrane potential at steady state, which is not easy to perform.

For in vivo recordings the *extracellular recordings* can be used. It consists of the recording of electric signal by means of microelectrodes placed into different brain regions. It allows recordings as close as possible to the physiological state. This technique presents a much specific signal than mass action potentials recordings (*EEG*) because the microelectrodes are able to record a smaller surrounding's electric signal. It allows easily localizing and monitoring single action potentials using a specific signal treatment. The *Single-Unit Analysis* is one of signal treatment carried out in the extracellular recordings.

The electrophysiological measurement techniques contribute to the understanding of the most complex and mysterious organ that our body can hide, the place where our conscience and all sensations take place: the brain.

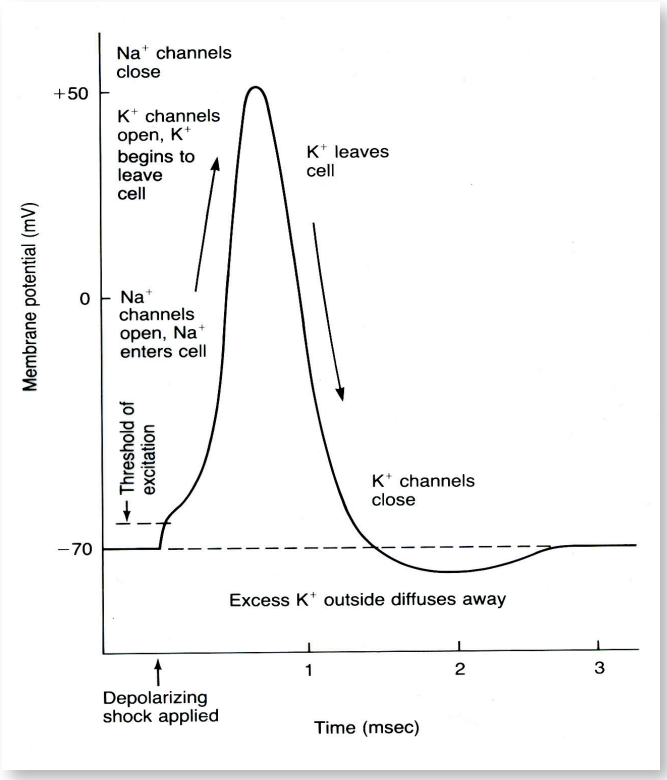

Figure 1. Graphical representation of an *Action Potential* as recorded in neurons. Recordings are made by mean of a patch clamp. Here the membrane potential is drawn as a function of time. A first modification of membrane polarity (i.e: due to a cell activation by an other cell, a mechanical stimulus, intracellular reaction, etc.) brings polarity to a certain threshold at which voltage-sensitive Na-channels open and let Sodium invade the cell. This brutal ion movement increases the membrane potential. With this *depolarization,* K-channels open and the outflow of positive charges through the membrane permits *repolarisation* with a *hyperpolarisation* phase (courses.washingt-on.edu).

3. The mammal brain and cortex

The embryological development of the brain is characterized by its division in five major parts. The forebrain is issued from the development of the two rostral parts of this division, the Telencephalon and the Diencephalon, while the three other subdivisions will develop themselves into brainstem and the cerebellum.

The surface of the telencephalon is covered by a thin layer of cells called the cerebral cortex, which is characterized by an architectural arrangement of its cells bodies into distinct horizontal layers (4 to 6 layers depending on the area of cortex). In each layers, different types of neurons can be distinguished on the basis of their morphology (pyramidal, granular, etc.) and/or their function (excitatory vs inhibitory). The different aspects of all layers (relative thickness, cell density or population, etc.) as well as their number allowed Korbinian Brodmann to divide the brain cortex into 52 cytoarchitectonic areas (*Figure 2, left*).

In the cortical areas, it is important to distinguish between *primary projection areas* that receive or send signal from/to periphery and the *secondary cortex areas* that receive and send information from/to the primary cortex areas. Areas 3, 1 and 2, anatomically located in the postcentral gyrus of the parietal lobe, make up the somatosensory cortex in humans (*the primary sensory cortex; SmI*). These three areas contain neurons that project on secondary somatosensorial areas (areas 5 and 7) (*Figure 2, Right*).

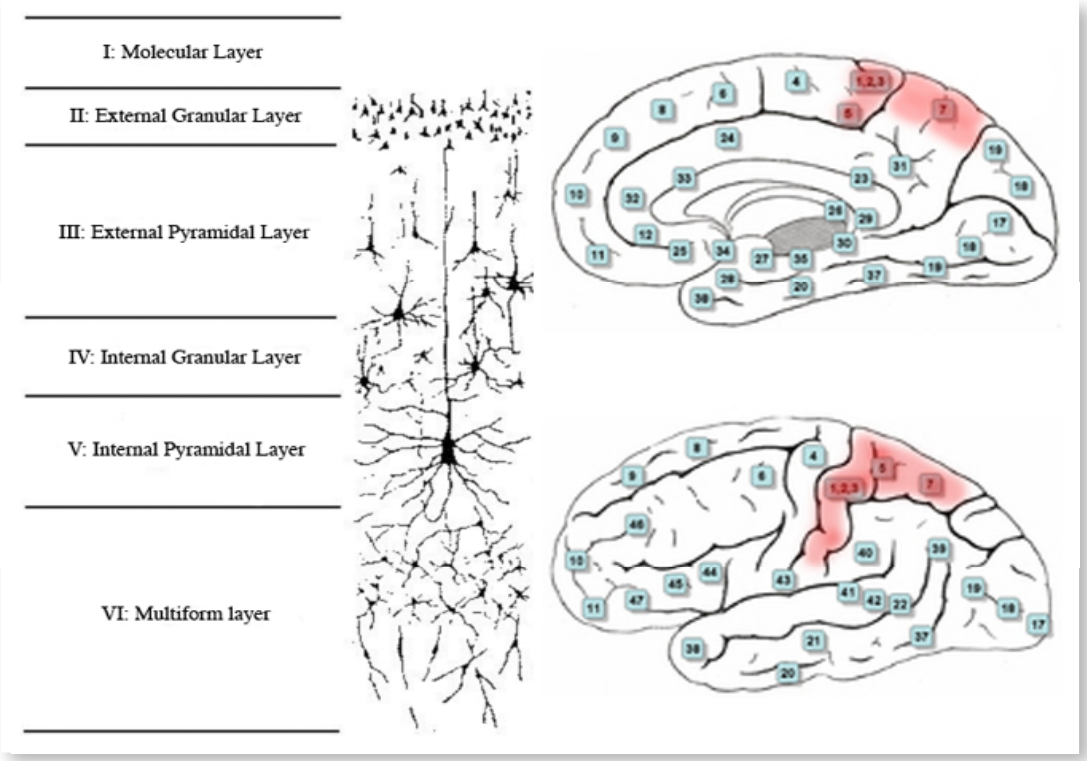

***Figure 2. Left**:* Arrangement of cerebral cortex in distinct layers. Layers II & III are also called supragranular layers and V & VI infragranular layers. ***Above right**:* Medial view of right human hemisphere. ***Right, under**:* Lateral view of left human hemisphere. These two last images show location of the 52 cytoarchiteconic areas defined by Brodmann. Somatosensorial areas are shown in red. Areas 3, 1 and 2 are located on the parietal cortex on the postcentral gyrus. Areas 5 and 7 are located on the posterior parietal cortex (sbirc.ed.ac.uk and fr.aca-demic.ru).

4. The somatosensory system

Life is only possible because organisms can interact with their environment. Different brain regions treat the information received from the environment and form the so-called sensory system that includes the auditory, visual and somatosensory cortexes.

The somatosensory system is characterized by peripheral neurons innervating receptors in the skin, muscles and joints that are communicating through different specific relays with the controlateral brain cortex (mostly in area 3 of the *SmI*). The primary sensory cortex, mainly receives sensory information of the body on its layer IV through projection from specific part of the ipsilateral thalamus. Integration of the signal mediated by reciprocal projections between *SmI* and areas 5 and 7, allows the treatment and integration of sensorial information and leads to a conscious perception of the environment.

The sensory information arrives to the *SmI* with a topological organization related to the distribution of the different sensory receptors of the body. A systematic correspondence between peripheral receptors of different body regions with specific areas in the *SmI* is created. Legs and trunk are represented close to the median line, while arms and hands are laterally represented on the *SmI*. This specific correspondence is called *somatotopy* (*Figure 3, left*).
The importance of each body part cortical representation depends on its peripheral density of innervations. In humans, lips and hands possess larger representation in the *SmI* compared to legs or trunk (*Figure 3, right*).

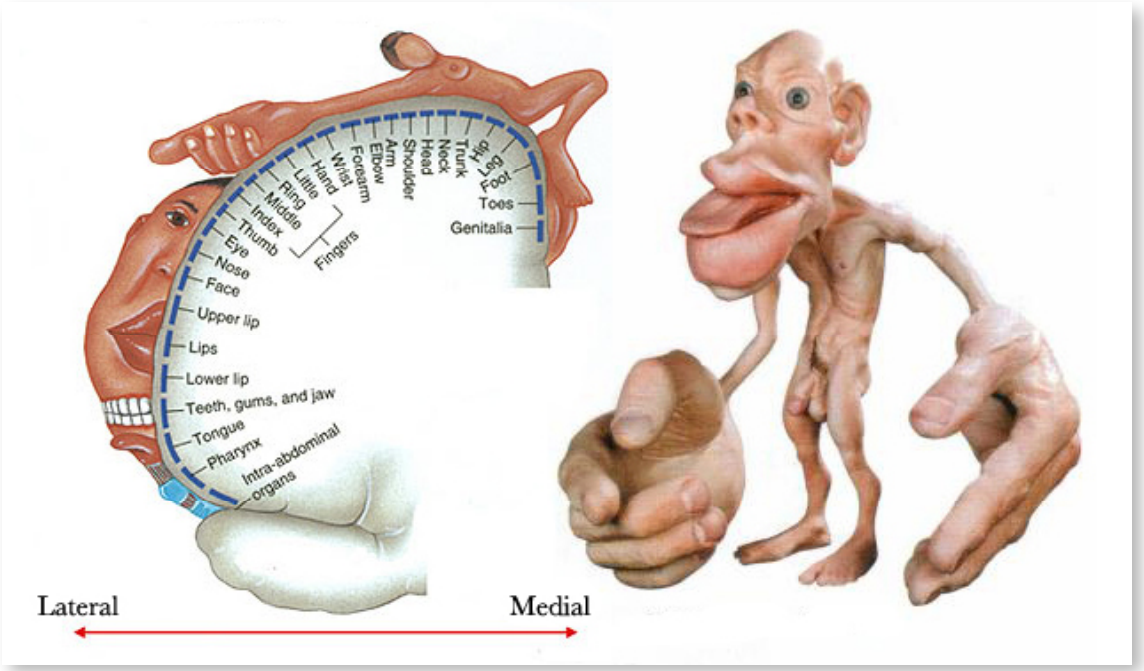

***Figure 3. Left**:* Somatosensorial map upon the human *SmI*. Caudal parts of human body are located medial while cranial parts lay on the lateral part of *SmI*. ***Right**:* Representation of the sensorial Homunculus. Relative density in sensorial peripheral innervations is represented. The size of the cortical corresponding region is directly proportional to its innervations (neurocritic.blogspot.com).

5. The whisker sensory system of rodents

5.1 From whisker to cortex

Whiskers or vibrissae are specialized hair located on the nose of multiple mammalian species in a region called whiskerpad. Each whisker contains a follicle on its base with mechanoreceptors sensitive to movement and follicular muscles that permit movement. In mice the whiskerpad is made up of five rows of large whiskers (A to E); each row is composed of four arcs. Caudally, the whiskerpad is composed of four straddlers (α, β, χ, δ). Near the snout are found some smaller whiskers, with less innervated follicles (*Figure 4*).

A follicular nerve independently innervates each follicle of the whiskerpad. These follicular nerves join the infraorbital nerve, a branch of the trigeminal nerve. Trigeminal mechanosensory neurons emerging from each follicle are exclusively sensitive to the movement of the associated whisker.

The axons connected to each whisker follicles and contained into the trigeminal nerves are converging on parts of the trigeminal nuclei sensory complex in the brain stem. From these nuclei, projections go straight to the *ventrobasal nucleus* (*VB*) and in the medial division of the *posterior nucleus* (*POm*) of the controlateral thalamus. The *thalamo-cortical* (*TC*) projections leave the *VB* to join the *SmI* where they arborized and make excitatory synapses, mainly in layer IV, but also in layer III and in the border between layers V and VI. Somatotopy is respected in the trigeminal nuclei by cytoarchitectonic structure named *barrelettes* and in the *VB* by a *barreloids* structure.

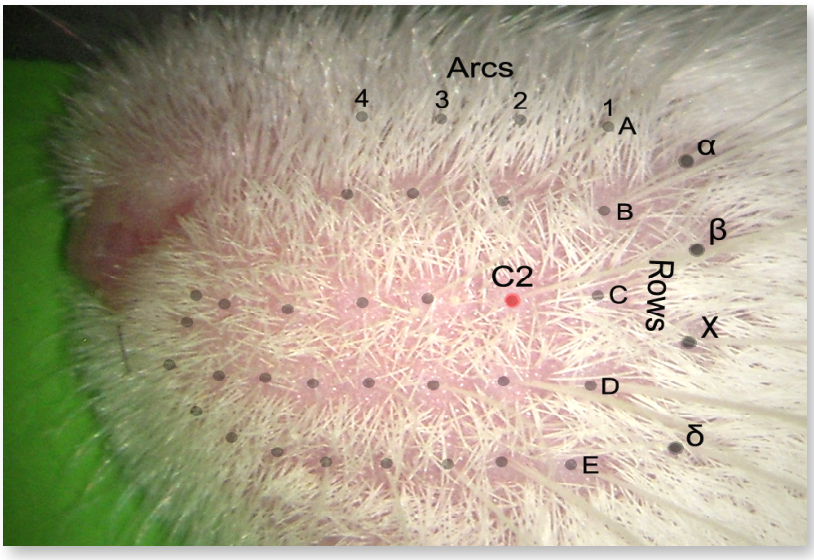

Figure 4. Representation of the left whiskerpad organization in the mouse. Each whisker follicle is shown by a grey dot. The follicles are arranged in rows (A to E) each of them composed or four arcs. Four straddlers are located caudally.

5.2 The barrel cortex

Rodents use their whiskers for the exploration of their surrounding environment and for the judgment of different surface textures. It though involves a huge numbers of facial whisker sensory receptors. As shown above the size of the cortical representation of a body region on the somatosensory cortex is proportional to its peripheral innervation density. This explains why, in mice, the cortical field dedicated to facial whiskers takes up one third of the total surface of *SmI* surface.

Barrels are discrete cytoarchitectonic neuron clusters located in layer IV of *SmI*. Each barrel receives most of its input from a single whisker on the controlateral face. The size of different barrels is thus specific to the density of myelinated sensory fibers innervating the correspondent whisker follicle. The specific region in *SmI*, containing all these barrels, is called *barrel cortex*. The part of the barrel cortex devoted to the largest whiskers (row A to E) defined the *posteromedial barrel subfield region* (*PMBSF*, *Figure 5*).

From a histological point of view, these layer IV clusters were termed barrels because of their three-dimensional structure. If a cut is made tangentially to the surface of the brain, these structures can be described as oval ensembles made of granular neurons. A richer population of cells compared to the center characterizes the border of barrels. Each barrel is surrounded by a depleted cell region or septa.

As shown above, thalamic projections terminate mainly in layer IV of the *SmI*, which contains the barrels. After their activation, layer IV neurons relay the signal to layers II&III. Layer III is then the source of long intrinsic descending connections with layers V and VI. This flow of vertical cortical activity defines, in a functional way, the *cortical columns* (Valverde, 1986). The barrels can be seen as a morphological identifiable component of this functional structure (Woolsey and Van der Loos, 1970). Most of the synapses present in a cortical column arise from intrinsic projections, rather than from the thalamus or distant cortical areas (Douglas and al., 1989; Douglas and Martin, 2007). Each cortical column is heavily connected vertically inside with its own perimeter, but is also connected horizontally with more or less distant columns so that the input arriving at a column is able to trigger different columns.

The whisker inducing the fastest and powerfulness neuronal response in a specific barrel is called *principal whisker* (*PW*). For example, cells in barrel C2 are excited quickly (6 to 10ms latency) and powerfully (1-2 spikes per stimulus) by deflection of whisker C2. As this response depends upon direct inputs from the thalamic ventral posterior medial nucleus, it is convenient to call whisker C2 the *center receptive field* (*CRF*) of barrel C2. Deflections of neighboring whiskers (e.g., Cl, C3, D2, or B2, the *surrounding whiskers*; *SW*) excite cells in barrel C2 less strongly and at a longer latency (20 ms on average). Since a separate pathway of intracortical inputs from surrounding barrels mainly generates the response to these whiskers, the neighboring whiskers are referred as the excitatory *surround receptive field* (*SRF*) of barrel C2. It is important to notice that columns are more strongly interconnected within a row than those in different row: this contributes to the fact that *SW* positioned within the same row as the *PW* (in previous example, C1 and C3) elicited strongest and fastest response compared with arc whiskers (B2 and D2).

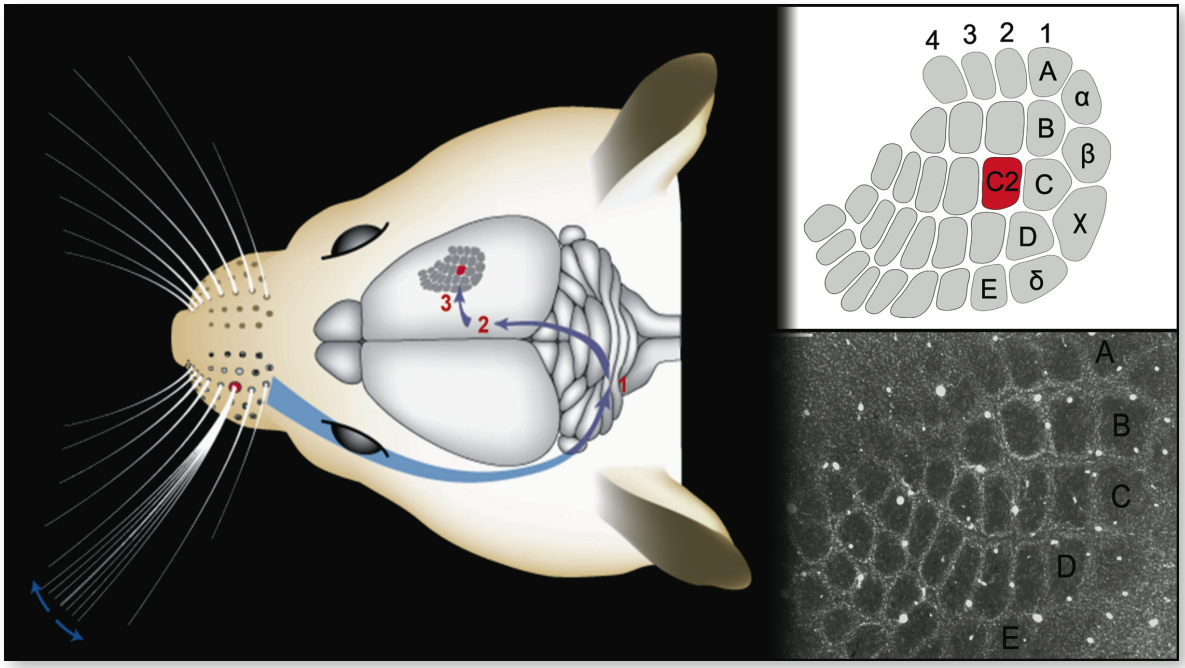

Figure 5. Left: After whisker stimulation, the signal is first conduct into the trigeminal nuclei sensory complex in the brain stem (1) then it relay on the controlateral thalamus (2) that send direct projections to the *SmI* cortex containing the barrels (3). ***Right:*** Schematic and histological representation of the *PMBSF* if a section is made tangentially in layer IV of barrel cortex. As a result of strict somatotopy, barrels are arranges in rows and arcs and are named according to their principal whisker. When C2 whisker is stimulated the strongest response will be recorded in the C2 barrel. Less strongest and different response can also be seen in C2 when surroundings whiskers are stimulated showing that connections exist between barrels (extracted from G. Knott).

Thalamocortical terminals in layer IV excite both excitatory and inhibitory neurons. Their function is not as well known as those of the excitatory ones. For a long time, it was assumed that inhibition was a single, homogeneous process, but some studies have shown a wide variety of inhibitory interneurons (Peters and Jones 1984; Mountcastle 1998), each of them having its specialized role. These neurons will induce a flow of inhibition, which will directly follow the excitation flow along its intracortical course. This inhibition limits both temporally and spatially the spread of excitation during whisker stimulation. It is thus important to consider that an important part of resulting signal to whisker stimulation results from this inhibitory wave, despite the fact that it is not directly obvious in extracellular recordings.

6. Overview of carbon fiber microelectrode signal processing

6.1 Carbon fiber microelectrodes

Multiple types of microelectrodes are used to record cortical activity. Carbon microelectrodes are preferred in neuronal electrophysiological recordings because they are easier to produce than other type of electrodes and are characterized by a very low signal-to-noise ratio.

To create such an electrode, a carbon fiber of about 7 micrometers diameter is inserted, using a microscope, into a borosilicate glass micropipette. To facilitate the insertion of the carbon fiber, the micropipette is filled with acetone. The pipette containing the carbon fiber is placed into a microelectrode puller leaving in the end a pointed micropipette with in its tip a protrusing microfiber. The exceeding of fiber is cut back with scissors to about 1 cm distance from the edge of the glass. The electrical connection to the carbonfibre is made with an electric wire, covered by silver-conducting painting, inserted on the other side of electrode. The carbon fiber is then sharpened micrometer from micrometer using a spark-etching process where a high voltage current being generated between the electrode and a brass wire leads to small electric arcs, or sparks, and to the erodation of the fibre. With this method, carbon is sculpted into a peak of approximately 7 micrometers long sticking out from the glass (*Figure 6, above right*).

These carbon microelectrodes are characterized by their low impedance (1-5 MΩ) allowing recordings of the signal with a large frequency range. This signal, processed by specific filters and modules arrangement, allows us to target the cortical activity of our interest.

During the experiments, the electrode is introduced, using a mechanical microdrive (*Model S-11, 10-μm precision; Narashige Instruments, Tokyo, Japan*), into the barrel cortex. An electrode, made of an electric wire, is placed on the scalp to serve as reference (*Figure 6*).

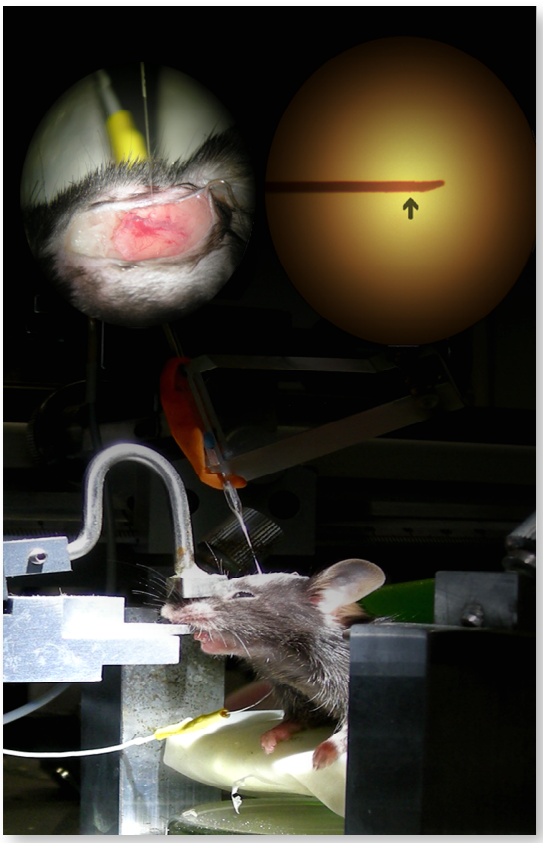

Figure 6. Microelectrode placement during the experiments.
Under: Anesthetized mouse is placed on headholder with a mechanical microdrive keeping the electrode in the cortical layer of interest. A continuous flow of oxygen is coming out in front of its nose.
Above left: Close up view of electrode placed into mouse brain. Note the reference electrode place on the scalp.
Above right: Microscope view of a microelectrode tip after spark-etching. The arrow shows the end of glass. During sparking, the purpose is to sharp the tip of the carbon fiber to obtain a pointed edge allowing easier recording of a single cell signal.

6.2 Impact of mice anesthesia

As recordings are more difficult on awake animals, anesthesia represents an essential part of the experiments. The principal anesthesia used in acute physiological in vivo experiments is urethane preparation. This anesthesia, which anesthetic action mechanism's is still unknown, is preferred in barrel cortex electric explorations because it offers a better stability through the course of hours (Armstrong-James and George, 1988).

This anesthesia is known to specifically modify the somatosensory activity compared with an awake state (Simons and al., 1992). An increase of latencies to peak response (the time between stimulation and the peak response) can be observed on *SW* deflections under urethane, while it don't influence latencies of *PW* stimulations (*Figure 7, above left*). Urethane also influences spatial cortical representation; in awake rats, receptive fields are smallest in layer IV barrels compared to anesthetized rats. Not only the time and spatial parameters of *SmI* response are affected by urethane; spontaneous activity levels in awake animals are twice those observed following induction of urethane. The anesthesia also typically increases the amplitude of cortical responses to whisker deflections. This represents an advantage of urethane on awake state with a higher response to stimulation/spontaneous activity ratio.

Experiments have been carried out on the influence of different states of urethane anesthesia on sensory cortical processing (Erchova and al., 2002). They showed that cortical spontaneous activity presents several changes in firing pattern depending on the depth of anesthesia. With the increase of this one, neuronal bursts (a correlated group of neuronal action potentials) rate decreases, as does the overall action potential rate. On the other hand, bursts duration increases and the proportion of spikes that occurs within bursts increases (*Figure 7, right*). Neuronal excitability is clearly modified and large populations of cortical neurons become bound together in cyclic waves of hyperpolarization and depolarization (Steriade and al., 1993) and *burst* together. These findings are important when we carry out experiments based on whisker stimulations because the burst state has a direct impact on single neuron response to whisker stimulation. In a general way, the best neuronal response to stimulation occurs mainly during burst onset and less during burst cessation. This could partly explain the fluctuation of neuronal cortical response to identical external stimuli observes sometime in the same animal during measurements.

Experiments have also explored how the depth of anesthesia affects whisker representations within barrel cortex. At the light stage, cortical activity, evoked by single-whisker stimulation, appears in a cortical field consisting of one central barrel-column and a set of surrounding one (Petersen and Diamond, 2000). At the intermediate and deeper stage, the cortical area engaged by the whisker stimulation decreased, as each whisker became an effective input for only a single corresponding barrel-column, interaction between barrels appearing to be impossible (*Figure 7, under left*). This is also an important fact to consider when testing a response of a specific barrel to stimulation of surrounding whiskers.

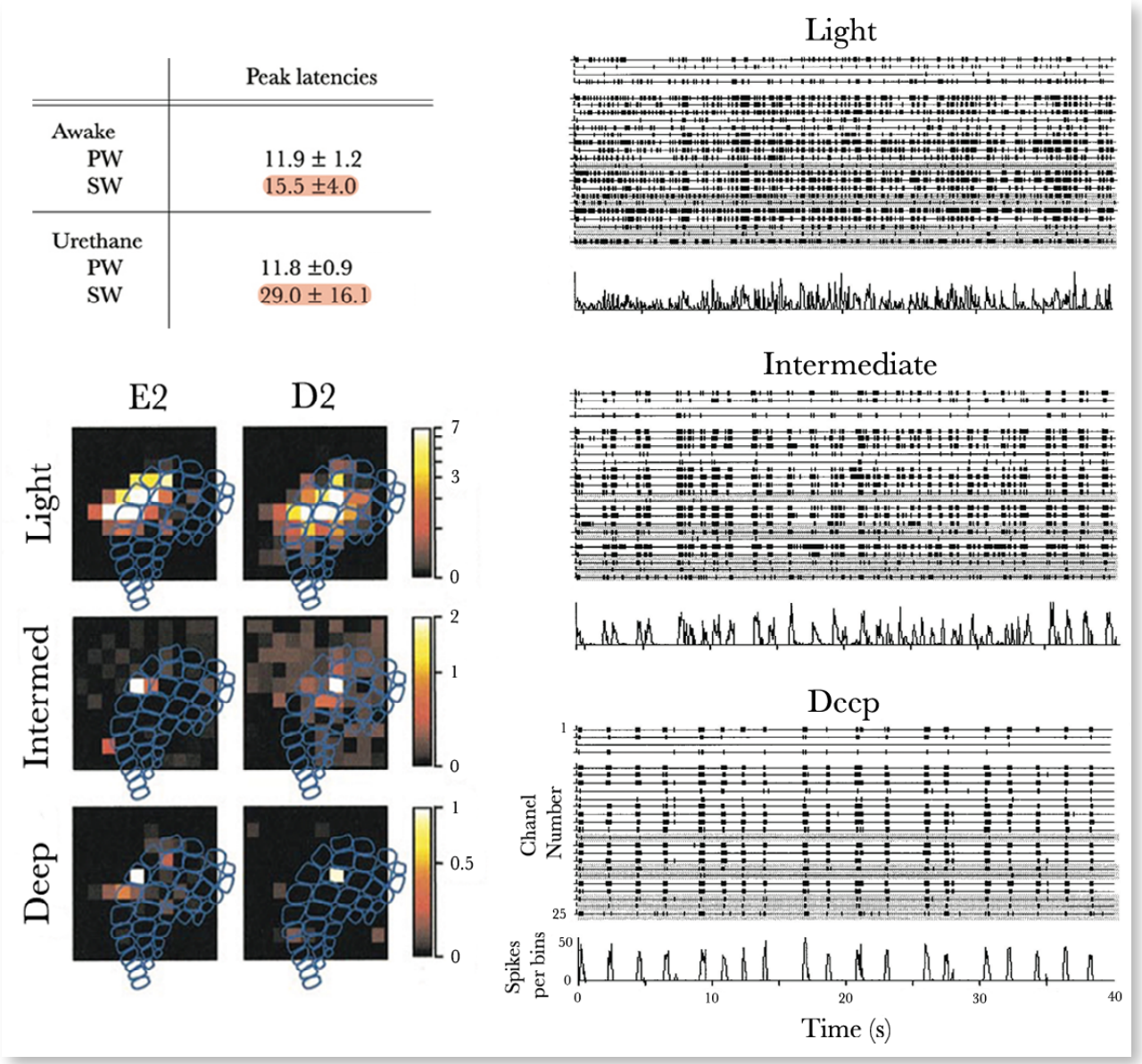

Figure 7. Above left: Peak latencies under awake and anesthetized state to *PW* and *SW* stimulation. Note the influence of urethane on *SW* latency (red) but not on *PW* latency. Numbers are in milliseconds ± 1*SD*. ***Right:*** Effect of light, intermediate and deep anesthesia on barrel cortex spontaneous activity recorded simultaneously at 24 electrodes. Light anesthesia is performed with an intra-peritoneal injection of 1.5g urethane per kilos body weight and is characterized by the absence of withdrawal from a pinch applied to the forelimb and the presence of corneal and eyelid reflexes. Intermediate and deep anesthesias are achieved by administration of supplemental doses of urethane (20% of the initial dose) each time. See how the firing patterns are changing progressively at single channels, as did the degree of synchronization across cortical sites; with increasing levels of anesthesia the neural bursts on different channels became increasingly synchronized. ***Left, under:*** Change in the cortical representation of individual whiskers across states of anesthesia. The response maps are derived from a 10 to 10 electrode array and are shown superimposed upon the barrel cortex map derived from the experiment. Responses to whiskers E2 and D2 stimulations are represented. Note that if the awake state was represented, receptive fields will be smallest than the light anesthetized state. The response magnitude scales for the whisker representations are logarithmic and differ in maximum values in the three stages (Simons and al., 1992 and Erchova and al., 2002).

6.3 Signal processing

When an electrode is placed into the cortex region of interest, the electric signal in its original state is difficult to interpret. It corresponds to the extracellular potential composed of the electric activity of cells close to the tip of the electrode from the global activity of distant brain structures. We

process it through series of filters and a signal discriminator to finally isolate specific patterns of interest. The treatment and analysis of the neuronal response is therefore possible.

6.3.1 Single-Unit Analysis (SUA)

The *Single-Unit Analysis* permits to study the extracellular electric signals of a single cell. The isolation of a single cell signal involves first the use of amplification medium and selective filters set on relatively high frequencies (800-1'500 Hz). Then, the signal has to be discriminated from global activity by mean of a discriminator. Everytime the cortical signal corresponds to the shape of a specific neuronal action potential, a dot is generated on time line. This allows to extract the difference specificity of one cell response, from latency between whisker stimulation and response, to magnitude of the response after stimulation compared with its spontaneous activity, through analysis of the time distribution of the response after stimulation (*Peri-Stimulus Time Histogram; PSTH*).

The limitation of this technique is that it permits to observe the response of a single cell that is not necessarily representative of the majority of the layer. Unmanageable sample sizes are therefore required for answering complex questions, such as interaction and response distribution depending on time between distinct cortical layers. We describe here two different techniques we used to discriminate signal.

6.3.1.1 The waveform window discriminated signal

After the amplification and filtering, the signal can be discriminated with a *waveform window discriminator* (*WWD*), which will select only a signal waveform passing first through a certain trigger level (depolarization of the cell) and then passing into a certain window of potential (repolarization/hyperpolarisation of the cell). Each time the signal passes through these two criterions a dot is generated on time line (*Figure 8*). The threshold and window levels are set manually during the experiments every time the electrode position is moved into the cortex.

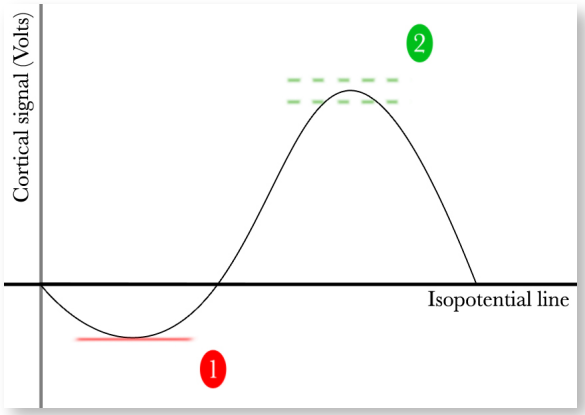

Figure 8. Schematic representation of cortical signal after its processing through the amplificators and filters. Every time a cell of interest generate action potentials, the window discriminator will create dots on time axis. Conditions for this are that signal must past first through a certain threshold (1) and then reach a defined window (2). Both parameters can be set manually to capture the specific response of one cell of interest. This technique is used as standard for single-unit measurements in the *DBCM*.

6.3.1.2 The Spike2 discriminated signal

Spike2 is a software (*Cambridge Electronic Design, UK*) allowing capture and analysis of various signals. It provides a function called the *spike shape discriminator* (*SSD*) that works in two steps.

During the first step, the templates detection is performed before stimulation. The spikes are detected by the input cortical signal crossing different triggers. There are two trigger levels, one for the positive-going and one for the negative-going spikes. The spike detection algorithm is as follows:

1. Wait for the signal to lie within half one of the trigger levels (baseline serve as reference). When it does, go to step 2.

2. Wait for the signal to cross either trigger level. If it crosses the lower trigger level go to step 3. If it crosses the upper level, go to step 4.

3. Track the negative peak signal value. If the signal falls above the peak, go to step 5. If the signal falls above half the upper trigger level, ignore further peaks (as for the second spike in *Figure 9*).

4. Track the positive peak signal value. If the signal returns below the peak, go to step 5. If the signal goes below half the lower trigger level, ignore further peaks.

5. Save the waveform template and go to step 1 for the next spike.

We manually set trigger levels during different measurements to detect the neuronal signal of interest.

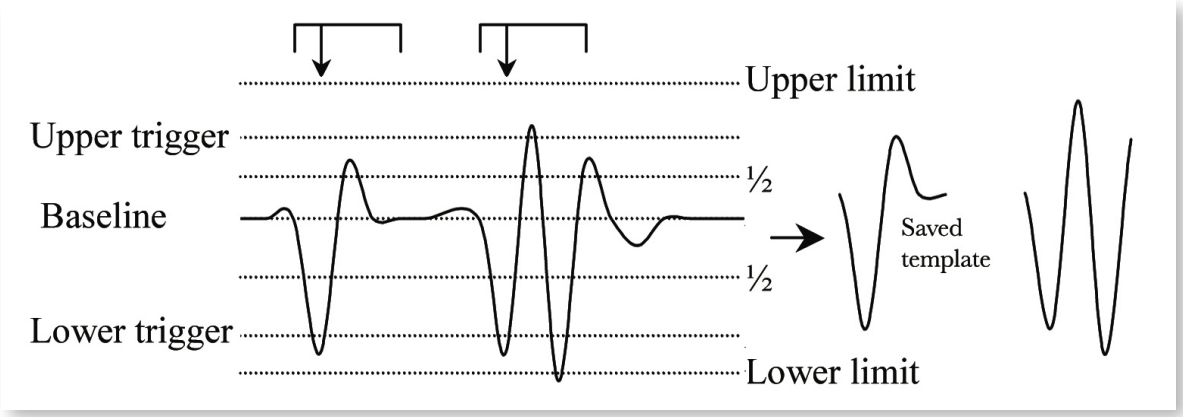

Figure 9. First processing of cortical signal by the *Spike2* software. The arrows on the top show the peak values. Each time the signal passes through the algorithm the waveform template is saved. All the saved templates are different one from another (extracted from *Spike2 for windows, manual*).

The second step of the *SSD* is performed during the whisker stimulation recording. Each previous saved template is defined by a number of points (that can also be set to get a sorting as specific and precise as possible). During the capture of the cortical response to whisker stimulation, each time the signal passes through a defined number of template points a dot is generated on time line.
The advantage of the *SSD* is that multiple templates can be used simultaneously during recordings allowing capture of multiple cells' signal in a single stimulation.

6.3.1.3 Data analyses

After having specifically selected the signal coming from the neurons, different presentations of the data are possible in the SUA. We display her some examples of the arrangements we frequently see in barrel cortex SUA explorations:

- Peri-Stimulus Time Histogram (PSTH)

The tempore spikes can be grouped together in a *Peri-Stimulus Time Histogram* (number of spikes function of time or spike per deflection function of time). In layer IV, *PSTH* is characterized by a specific temporal profile (Quairiaux and al., 2007, *Figure 10*). Neurons fire action potentials in

response to whisker deflection from 6ms poststimulus, reach a peak at 11ms (poststimulus epoch T1: 3-11 ms), and then gradually decreased to near spontaneous levels about 25ms poststimulus (T2: 12-25 ms). During the next 25 ms, spiking probabilities did not exceed the spontaneous level (T3: 26-50 ms). A rebound of activity takes place in the fourth epoch (T4: 51-100 ms), after which probabilities returned to the spontaneous level (T5: 101-200ms).

The *PSTH* recordings begin a 3ms poststimulus to avoid the electric noise generated by the whisker stimulator. They are very useful to compare poststimulus epoch changes in cell response to different previous whisker conditions (24 hours stimulation, non-stimulated, etc.).

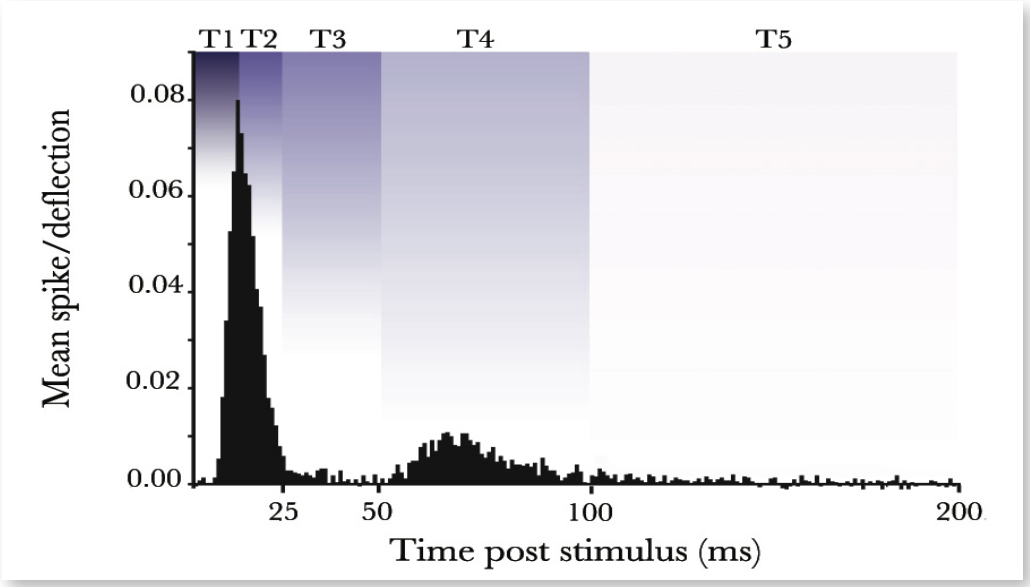

Figure 10. Example of *PSTH* created with the signal of 102 different cells response to PW stimulation in layer IV of column C2. Note the specific temporal profile of response with the different poststimulus epoch (Quairiaux and al., 2007).

- *Latency*

A parameter allowing us to distinguish different neurons type or in which layer of cortex the electrode is placed is the difference in latency response to a stimulus. To calculate it, the time of the first spike after the onset of whisker deflection is hold. Based on it, a median latency, interquantile ranges (q75-q25) and 10-90 percentiles can be calculated. It is important to notice that the latency of one cell, in addition to its type, is dependent of thalamo-, intra- and intercortical connections and as seen above, depends also of anesthesia.
In some studies, *modal latency* is calculated for comparison and analysis and is obtained by taking the time of the bin in the *PSTH* with the peak value.

- *Response magnitude (RM)*

The corrected response magnitude is the mean number of spikes evoked per deflection corrected for the spontaneous activity. It is calculated using the *PSTH* data contained in certain time period after the whisker deflection minus the number of spikes that occurred during a similar time interval before deflection. For our measurements, *RM* was calculated using the 3 to 100ms poststimulus period.

Practice

7. Aim of the work

The aims of the practical works were:

1. To get familiarized with intracortical recordings in an anaesthetized mouse.

2. To understand the value of quantification of response properties of neurons in rodents somatosensory cortex.

3. To compare the use of two different spike discrimination methods (*waveform window discrimination/Spike2 spike shape discrimination*).

8. Material and methodology

8.1 Mice sample

The recordings were performed on 12 adult pigmented mice (strain *C57/Bl*). Because two mice offer a poor signal, data was obtained from only 1 female and 9 male. These 10 mice were young adults between 2-3.5 month of age. Their weight was between 25-35g. For each measurement we used mice that had all caudal whiskers (long *PW*s and *SW*s). All animal handling procedures used for this study were previously approved by the Office Veterinaire Cantonal (Lausanne, Switzerland) in accordance with Swiss Federal Laws.

8.2 Anesthesia and surgery

The electrophysiological recordings were performed under urethane anesthesia (10% solution in distilled water; 2mg/g body weight, i.p.). After the urethane injection, mice received a subcutaneous dose of lidocain (0.1 ml; 1% w/v; Xylocain) above the parietal bone after which the animal was mounted in a stereotaxic frame equipped with a homemade headholder (see *Figure 6*) providing a continuous flow of oxygen in front of its nose. The body temperature was maintained at 37°C by a heating pad (Homeothermic Blanket System Harvard 50-7061, England). Under optical magnification, the scalp was incised and a craniotomy of the right parietal bone was realized with a small electric drill to expose a large part of the somatosensory cortex including the *PMBSF*. After stereotaxic placement of the electrode in the barrel of interest, the exposed region was covered with 1% agar dissolved in 0.9% saline. The depth of the anesthesia was continuously controlled using as criteria the absence of whisking reflex. Supplementary urethane doses (10% of the original dose) were given if necessary.

8.3 Electrophysiological Recordings

The data were recorded from C2 barrel in 9 mice and from C3 barrel in 1 mouse. The sample area was identified using stereotaxic coordinates and cortical response to manually deflected whiskers of the controlateral whiskerpad.
Subpial depth of each recording site was recorded. The recording sites were targeted to supragranular layers II&III (150-349μm), granular layer IV (350-479 μm) and infragranular layer V (480 μm and more).
The signal coming from the electrode placed in the barrel was amplified and processed by a Neurolog module arrangement (*Neurolog System, Digitimer, Welwyn Garden City, UK*). From the first

analog signal a single-unit signal was isolated, based on its amplitude and waveforms by means of a *WWD*, or by mean of the *Spike2 SSD* (see chapter 6.3.1.1 and 6.3.1.2).
For the *WWD*, the threshold and window levels were set manually for each measurement. The waveform window signal was then processed using the CED-Power 1401 interface (*Cambridge Electronic Design, UK*).
For the *SSD* the trigger levels were also set manually for each measurement. The waveform templates were saved before measurement, each of them were composed of 62 points. During stimulation, a spike matched with the templates when it had minimum 60% of the points in common. It is important to notice that the *SSD* method took time to handle and we felt comfortable with it only in the late recordings.
Spike2 recorded spikes with a maximum event rate set on 3'000 Hz for the *SSD* signal and 500 Hz for the *WWD* signal. An audiomonitor was coupled to the recording amplification circuit, allowing us to listen to patterns of voltage changes in brain activity.

8.4 Data analysis

Analyses were carried out using a homemade script written in *Spike2* software language. Data from responses to the *SWs* and *PWs* stimulations were treated separately.
The responses to stimulation were considered significant after having filled the following criterion. First, the poststimulus response magnitude (measured using the 3 to 200ms post-stimulus interval) was corrected for spontaneous activity as determined during an equivalent time period before the stimulus onset. The corrected response magnitude from the 3 to 200ms interval had to be equal or larger than 10 % of spontaneous activity. Finally, the number of spikes of the corrected magnitude had to be sufficient (more than 3 spikes in the first 100ms period) to determine a median latency.
The distributions of median latencies and corrected response magnitude (*RM*) were tested for normality (*Normal Quantile-Plot*). In approximately half of the case normality was rejected; we therefore use median latencies interquantile ranges as well as 10–90 percentiles, to analyze and compare those parameters. The median latencies of each cell were collected and used to calculate latency box-plot for each layer. The median corrected *RM* was also calculated for each layer. Spike times were collected into 1ms bins to help building *PSTHs* for each layer. The differences between results were considered significant following a *Mann-Whitney* statistical test (a nonparametric test for the significance of the difference between the distributions of two independent samples, we had to assume that data were independent) with a 5% confidence level. The test was carried out using the *Vassar college* online tool (*VassarStats: Website for Statistical Computation, http://faculty.vassar.edu/lowry/webtext.html*).

8.5 Whisker deflection procedure

C2 and surroundings whiskers (C1, C3, B2, D2) and for one mice C3 and surrounding whiskers (C2, C4, D3, B3) were deflected one at time. First, the whisker was trimmed to about 3cm length and insert into a thin borosilicate glass tube attached to a piezoelectric bimorph slab. The whisker stimulus consisted of an upward deflection of 3ms duration. The movement of the probe was evoked by square wave voltage pulses delivered by a high voltage stimulator (*Digitimer stimulator D59A; Digitimer Ltd, UK*) gated by the *CED-Power-1401* interface and *Spike2* signal generator. A systematic control was made to insure that the glass probe did not touch other surrounding whiskers during stimulation. The amplitude of the deflection was approximately of 1.43°, a value used as standard deflection in previous studies. Cortical responses were recorded upon a 50 repetitions of the whisker deflection at a 0.5 Hz frequency.

9. Results

9.1 Waveform window discriminator (WWD) results

The responses to *PW* of 26 cells were selected and recorded with the *waveform window discriminator* (19 in layer IV, 3 in layers II&III, 4 in layer V). In these cells, 24 of them were recorded after *SW* stimulation, 17 in layer IV (68 recordings for the four whiskers), 3 in layers II&III (12 recordings) and 4 in layer V (16 recordings).
100% of the cell in layer IV had a significant response to *PW* stimulation and 57% (n = 39) to *SW* stimulation; 32% (n = 22) to stimulation of *SW* whiskers in the same row than *PW*, 25% (n = 17) to stimulation of *SW* whiskers in the same arc. Layers II&III and V had both 100% significant response to *PW* stimulation and respectively 75% (n = 9) and 81% (n = 13) to *SW* stimulation.

Layer IV cells had a median latency of 11.0ms (p10 = 8.8; p90 = 16.2) to *PW* stimulation (n = 19) and 50.9ms (p10 = 22.4; p90 = 69.9) to *SW* stimulation (n = 39); 43.0ms (p10 = 20.5; p90 = 65.5) to whiskers in the same row (n = 22), 55.9ms (p10 = 30.8; p90 = 74.5) to whiskers in the same arc (n = 17).
In layers II&III, median latency was 17.0ms (p10 = 16.2; p90 = 23.4) to *PW* stimulation (n = 3) and 35.0ms (p10 = 19.6; p90 = 62.5) in response to *SW* (n = 9); 26.0ms (p10 = 19.6; p90 = 53.1) to whiskers in the same row (n = 3), 35.0ms (p10 = 27.5; p90 = 56.9) to whiskers in the same arc (n = 6).
In layer V, median latency was 22.2ms (p10 = 15.9; p90 = 27.9) to *PW* stimulation (n = 4) and 30.0ms (p10 = 24.8; p90 = 62.7) to *SW* stimulation (n = 13); 30.0ms (p10 = 26.2; p90 = 41.9) to whiskers in the same row (n = 13), 40.0ms (p10 = 27.0; p90 = 66.1) to whiskers in the same arc (n = 6).
The *PW* and *SW* latencies difference between the layers was not significant. *Figure 13* shows the distributions of the latency of *PW* responses as a function of cortical depth.

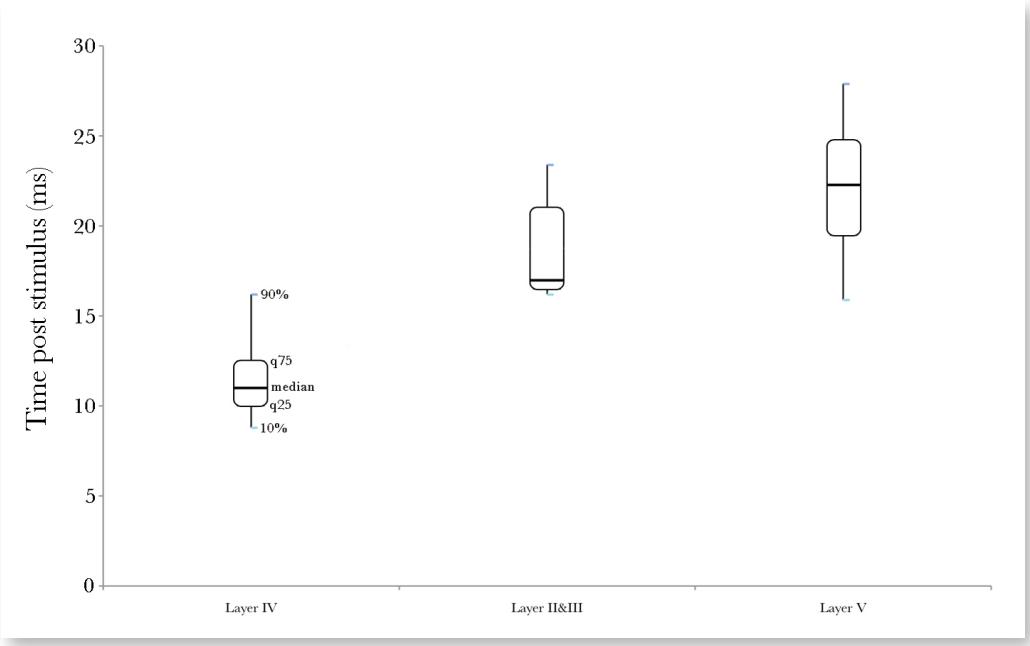

Figure 13. Box plots of *PW* stimulation median latencies computed for neurons in layer IV, layers II & III and layer V after waveform window discrimination. Interquartile ranges as well as 10–90 percentiles are represented.

Median corrected *RMs* in layer IV were 1.7 spike/deflection (p10 = 1.2; p90 = 6.0) in response to *PW* stimulation (n = 19), 2.4 spike/deflection (p10 = 2.4; p90 = 2.6) in layers II&III (n = 3) and 1.5 spike/deflection (p10 = 1.2; p90 = 4.7) in layer V (n = 4). The *PW-RM* difference between the layers was not significant. *Figure 14* illustrates the median corrected *RM* in layers IV, II&III and V to *PW* stimulation.
Corrected *RM* to *SW* stimulation were 0.2 spike/deflection (p10 = 0.1; p90 = 1.8) in layer IV (n = 39); 0.4 (p10 = 0.1; p90 = 2.2) to whiskers in the same row (n = 22), 0.2 (p10 = 0.1; p90 = 0.8) to whiskers in the same arc (n = 17).
In layers II&III corrected *RM* to *SW* deflection (n = 9) was 0.2 spike/deflection (p10 = 0.1; p90 = 1.0); 0.3 (p10 = 0.2; p90 = 1.7) to whiskers in the same row (n = 3), 0.2 (p10 = 0; p90 = 0.5) to whiskers in the same arc (n =6).
In layer V corrected *RM* to *SW* deflection (n = 13) was 0.4 spike/deflection (p10 = 0; p90 = 2.5); 0.4 (p10 = 0; p90 = 3.1) to whiskers in the same row (n = 7), 0.4 (p10 = 0.1; p90 = 1.3) to whiskers in the same arc (n = 6).
The *SW-RM* difference between the layers was not significant.

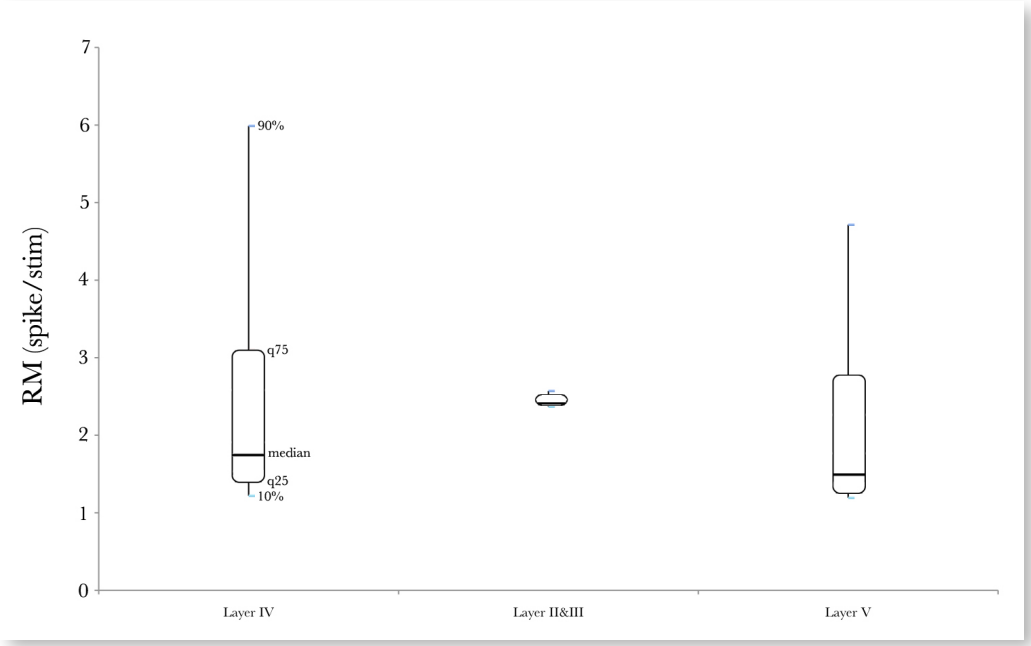

Figure 14. Median corrected *RM* with interquartile and 10-90% ranges for neurons in layer IV, layers II & III and V of barrel columns in response of *PW* stimulation and waveform window discrimination.

Figure 15 shows the mean *PSTHs* as calculated for the responses to *PW* stimulation per layers.

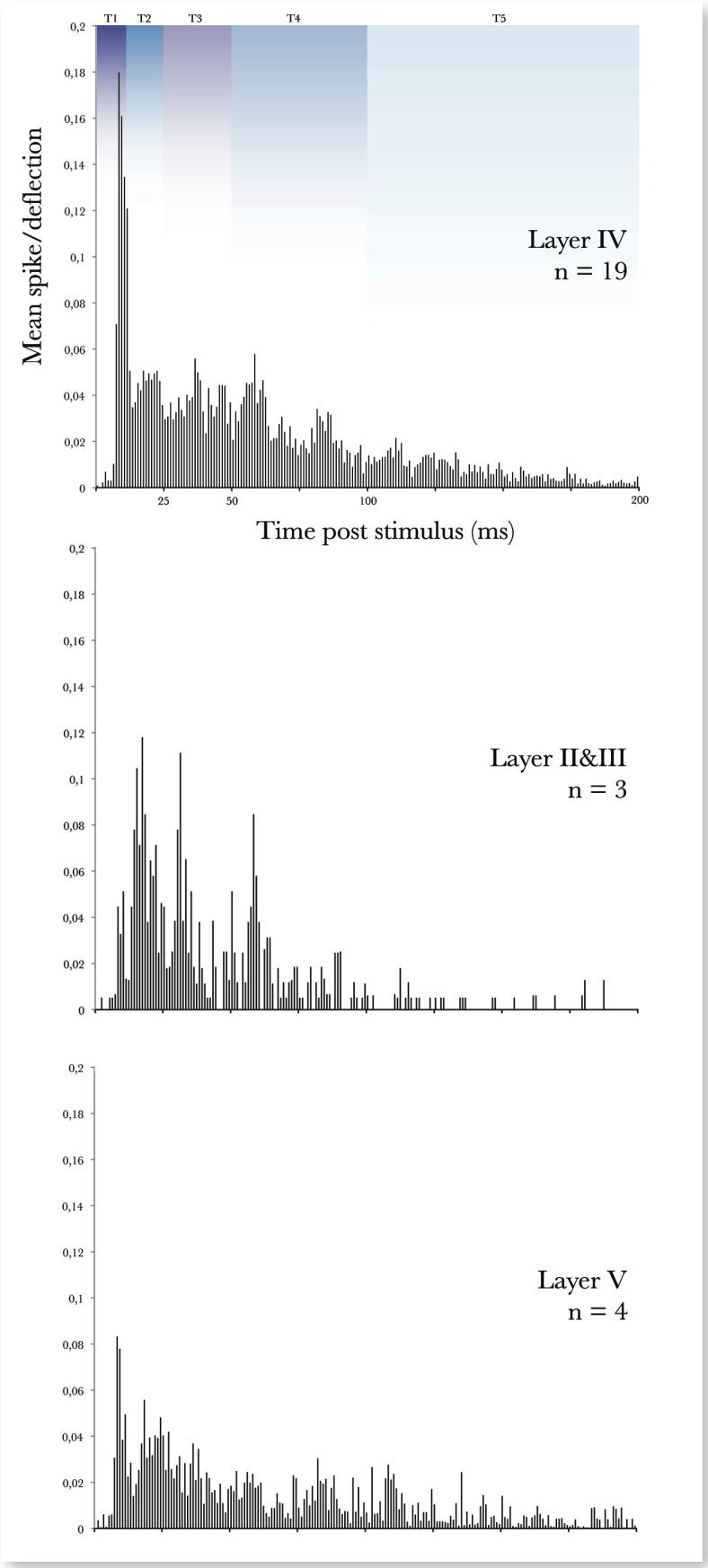

Figure 15. *PSTHs* for neurons responding to *PW* deflection in layer IV, layers II & III and layer V with waveform window discrimination. Epochs defined by Quairiaux are labeled on layer IV histogram and indicated using graded colors.

Figure 16 shows the mean *PSTHs* as calculated for the responses to *PW* stimulation per layer.

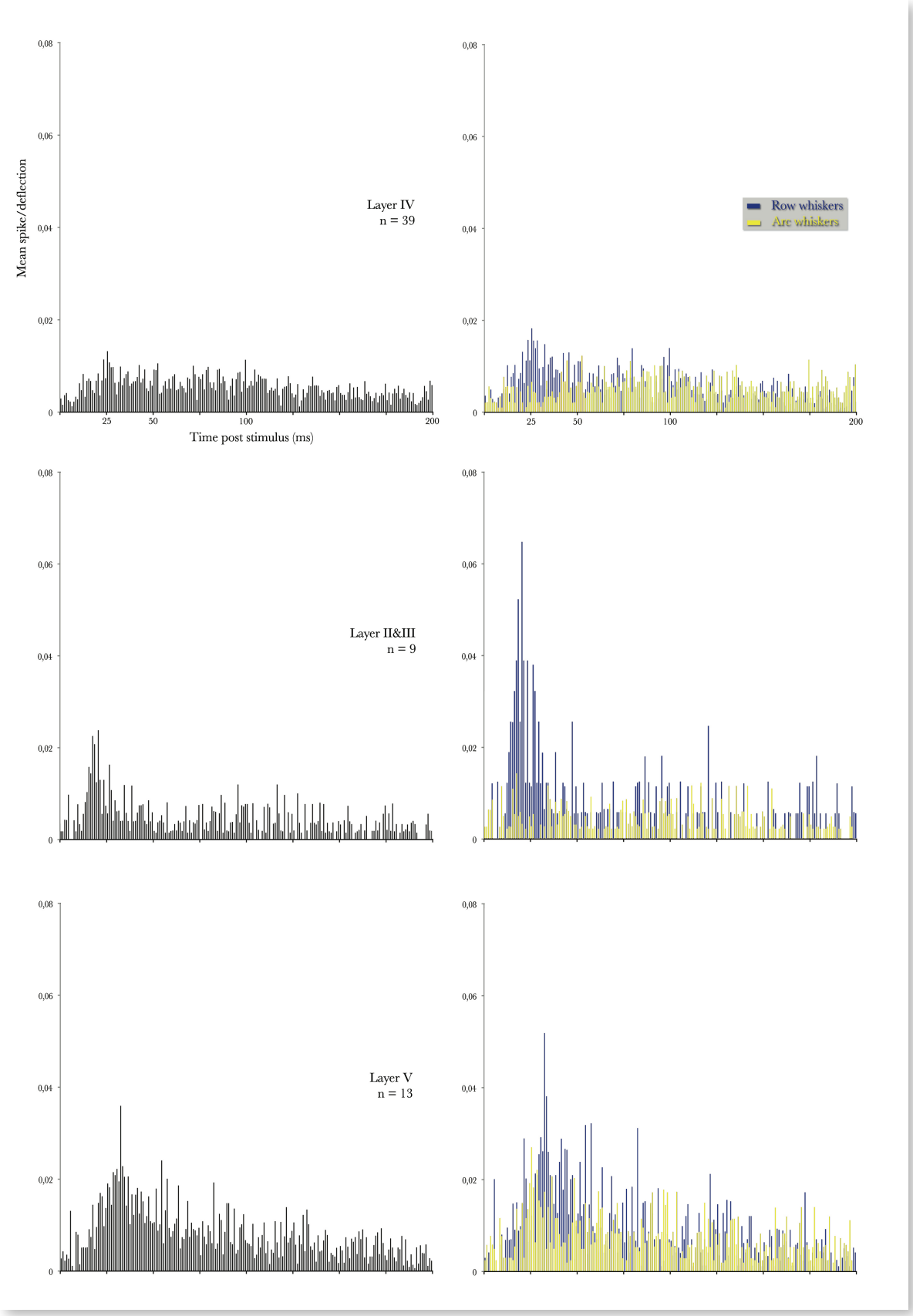

Figure 16. *PSTH* for neurons responding to *SW* deflection in layer IV, layers II & III and layer V with waveform window discrimination. Left column shows cumulative response to all *SW* stimulation. Right column shows response to *SW* located in the same row than PW (row C, blue) and to *SW* located in the same arc (row B and D, yellow).

9.2 Spike shape discriminator (SSD) results

The *SSD* was used on 24 recording site and allowed us to record 70 templates in which 94% (n = 66) had a significant response to *PW* stimulation.

The median latency to *PW* stimulation was 20.0ms (p10 = 9.8; p90 = 44) in layer IV (n = 49), 29.0ms (p10 = 17.8; p90 = 29.8) in layers II&III (n = 3) and 25.0ms (p10 = 27.5; p90 = 58.9) in layer V (n = 14). The *PW* latency difference was significant between layer IV and layer V (p = 0.04). The difference was not significant between layer IV and layer II&III and layer II&III and layer V. *Figure 17* shows the box plot of different layer response to *PW* stimulation when *spike shape discriminator* was used.

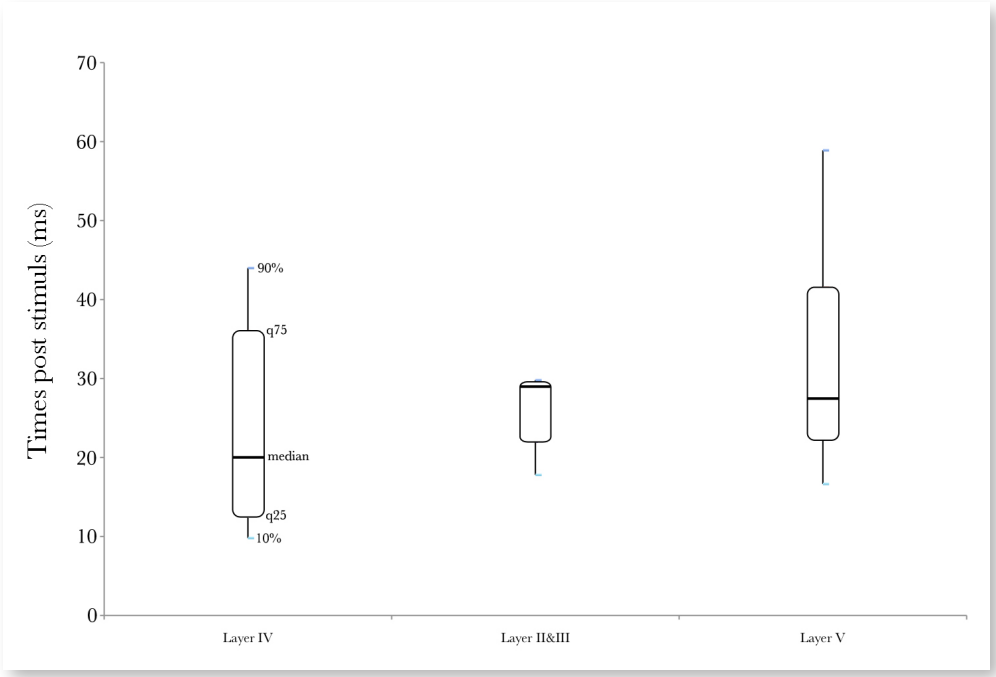

Figure 17 above, figure 18 under. Box plots respectively for median latencies and median corrected *RM* for layer IV, layers II & III and layer V after *PW* stimulation and *SSD* processing. Interquartile ranges as well as 10–90 percentiles are represented.

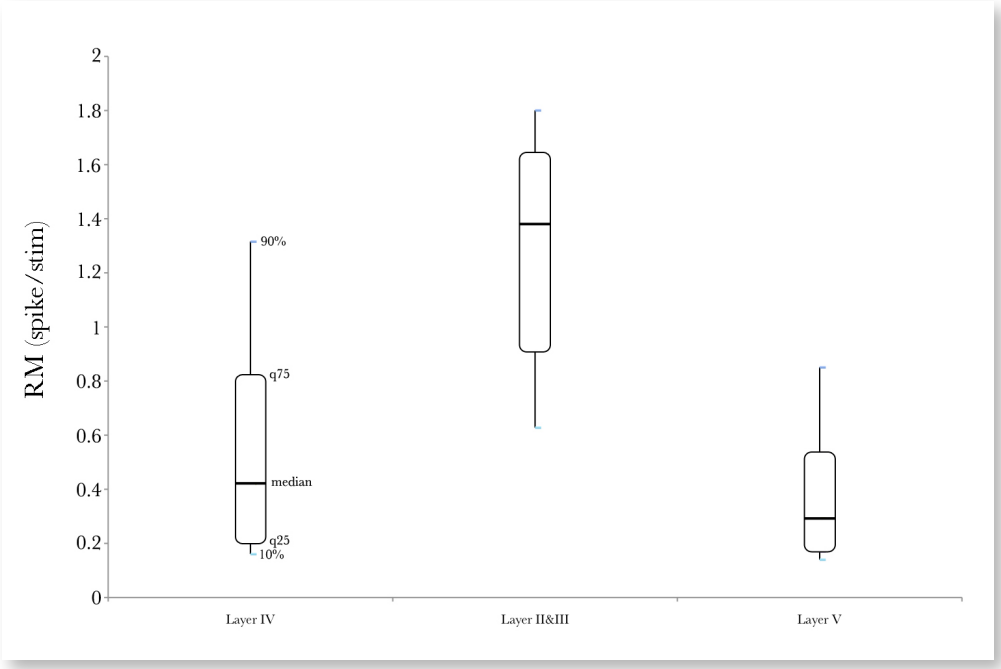

Median *RM* to *PW* deflection was 0.4 spike/deflection (p10 = 0.2; p90 = 1.3) in layer IV (n = 49), 1.4 spike/deflection (p10 = 0.6; p90 = 1.8) in layers II&III (n = 3) and 0.3 spike/deflection (p10 = 0.1; 0.9) in layer V (n = 14). The *PW-RM* difference between the layers was not significant. *Figure 18* shows the box plots of *RM* recorded with the *SSD*.

Figure 19 shows the mean *PSTHs* as calculated for the responses to *PW* stimulation per layers with the *SSD*.

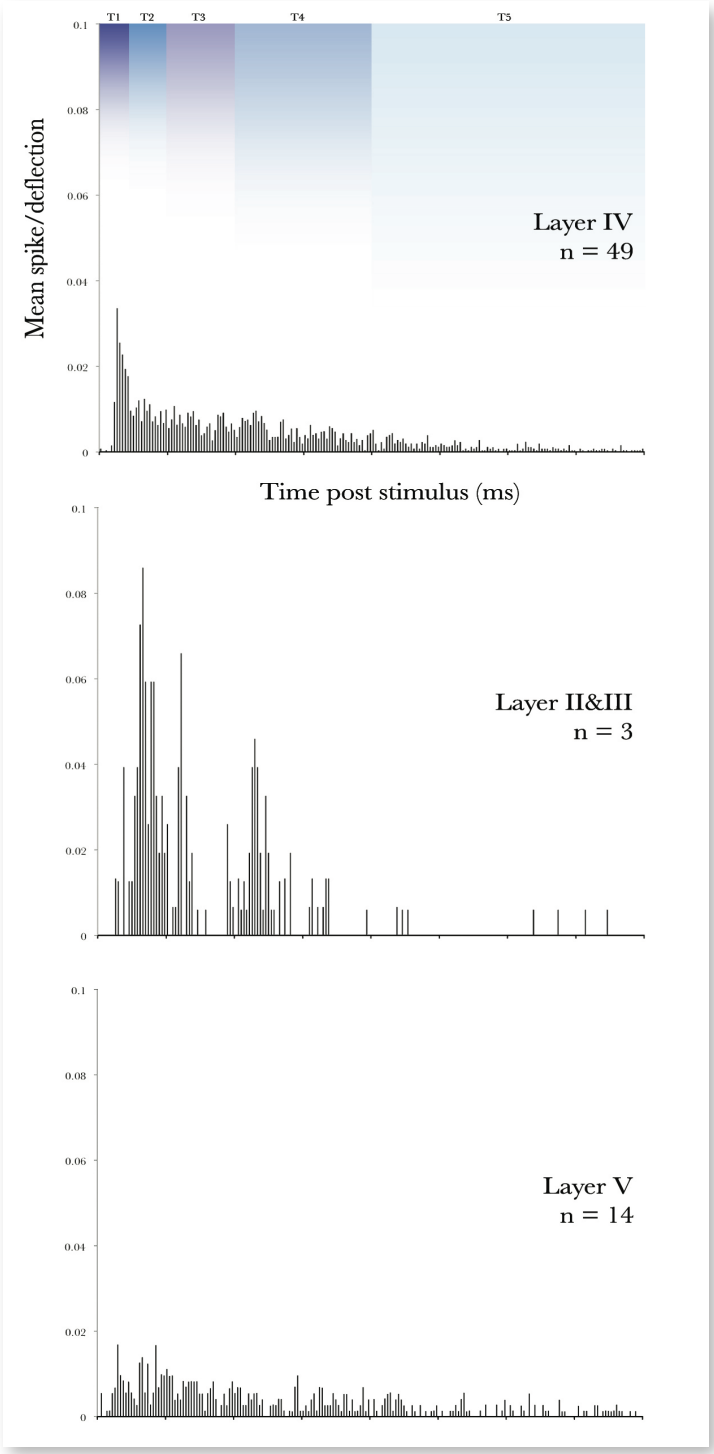

Figure 19. *PSTH* for the *SSD* signal responding to *PW* deflection in layer IV, layers II & III and V. Epochs defined by Quairiaux are labeled on layer IV histogram and indicated using graded colors.

9.3 Comparison between the WWD and SSD results

The median latency and *RM* were different between the two methods of signal discrimination. In all layers, *RM* value was smaller and latency was larger with the *SSD*. *Figure 20* compares the latencies and *RM* calculated for the two populations.

Latency (ms)	WWD	SSD
Layer IV	p = 0.0003 11.0 (p10 = 8.8; p90 = 16.2) n = 19	20.0 (p10 = 9.8; p90 = 44) n = 49
Layer II &III	17.0 (p10 = 16.2; p90 = 23.4) n = 3	29.0 (p10 = 17.8; p90 = 29.8) n = 3
Layer V	22.2 (p10 = 15.9; p90 = 27.9) n = 4	25.0 (p10 = 27.5; p90 = 58.9) n = 14
RM (spike/stim)		
Layer IV	p = <0.0001 1.7 (p10 = 1.2; p90 = 6.0) n = 19	0.4 (p10 = 0.2; p90 = 1.3) n = 49
Layer II &III	2.4 (p10 = 2.4; p90 = 2.6) n = 3	1.4 (p10 = 0.6; p90 = 1.8) n = 3
Layer V	1.5 (p10 = 1.2; p90 = 4.7) n = 4	0.3 (p10 = 0.1; 0.9) n = 14

Figure 20. Table showing the different values of median latencies an *RMs* in all three layers for *WWS* and *SSD* discriminations. 10-90 percentiles and sample size are notified. A red dot means the presence of a significant difference between values.

To understand properly how latencies and *RMs* were distributed in layer IV, with the two discriminating methods, we plotted their value function of their relative count. *Figure 21* shows the relative distribution of the median latencies and *RMs* in layer IV when the *WWD* and the *SSD* served as discriminator. As seen in *Figure 20*, the difference between the two discriminations was significant in layer IV.

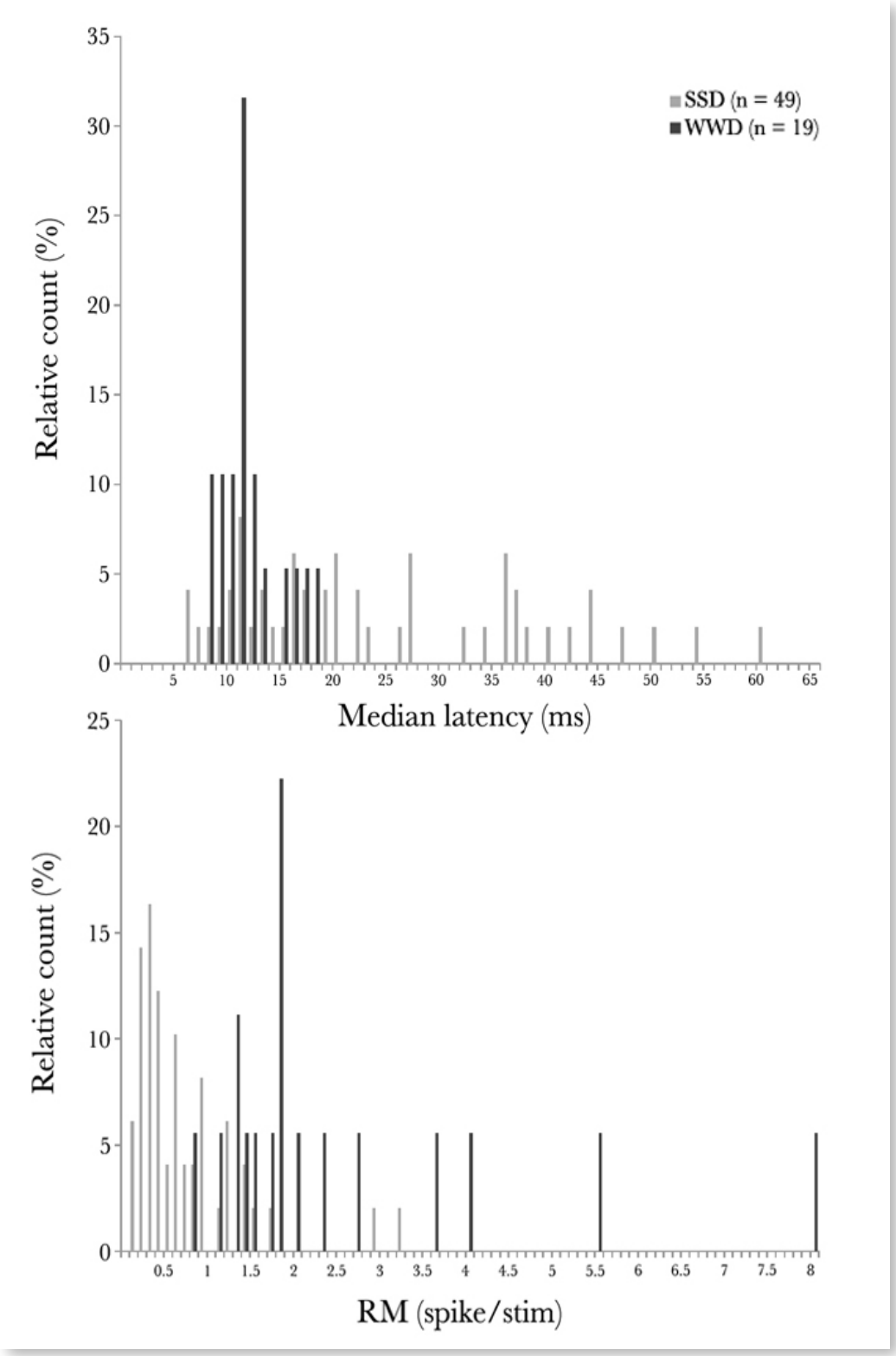

Figure 21. Relative distribution of latencies and *RM*s values in layer IV with the *SSD* and *WWD*.

10. Discussion

The median latency was significantly different in layer IV between the *WWD* and the *SSD* discriminated signal. If we look at *Figure 21*, we see that the *WWD* cumulated median latencies around 11ms (its median value) while the *SSD* discriminated scattered values (between 6 to 60ms) with no defined peak value. This temporal distribution of cell latencies with the *SSD* discrimination didn't correspond with the characteristic behavior of the cortical cells. The templates the *SSD* detected were probably not recording cortical cells. In opposition, the temporal distribution of *WWD* latencies fitted with previous *Single-Unit Analysis* performed in layer IV barrel cortex (Quairiaux and al., 2007). The lack of precision of the *SSD* in the recording of the latencies probably came from the setting used to discriminate signal. The latencies values were dispersed because *SSD* sorted signal (probably noise fitting with the templates) as action potential that the *WWD* for example didn't detect. The peak value was probably decreased with the *SSD* because signal that the *WWD* sorted as cell action potentials didn't fit with the SSD templates. In our study, the templates were composed of 62 points and to match with them signal had to pass through 60% of these points. Those parameters were chosen because they were described as standard for our kind of research in the *Spike2* user manual. We didn't try to vary them and this will have probably changed signal selectivity of the *SSD* measurement. If we look to the magnitude values of *Figure 21* we see, with the *SSD*, that *RMs* were gathered around a peak of 0.2-0.4 spike/stim (median = 0.4) and that the *WWD* signal peaked at 1.8 spike/stim (median = 1.7) but other surrounding values were dispersed. We cannot conclude on anything with these findings because of the imprecise nature of the *SSD* technique seen above. All we can say is that values difference was significant. The *SSD* and *WWD* showed difference in the layer IV *PSTHs* with an increased response magnitude with *WWD* during all post-stimulus periods. The ratio between the peak value (during T1 and T2) and the activity during late periods also seemed bigger with the *WWD*. Again, conclusions on *SSD PSTHs* are difficult because of the unknown signal origin.

The median latencies and *RMs* differences also appeared between the *WWD* and *SSD* discrimination in layers II&III and layer V, but no significant statistical difference had been shown. This came probably mainly from the limited size of samples in these two layers. The temporal profile of response in layers II&III showed difference in magnitude between the two techniques. However, we can see that the *three-peak profile* we see with the *WWD* was conserved with the SSD. In the layer V, as for layer IV, *SSD* shows a global response magnitude flattened with the extinction of the peak shape we see with the *WWD*. Here again sample size (particularly with the *WWD*) in addition to *SSD* signal quality limits conclusions.

The time distribution between layers of the *WWD* latencies in response to *PW* stimulation fitted with the wiring diagram of the somatosensory cortex where the peripheral information enters first layer IV (~11ms), then related to neurons in layers II&III (~17ms) and then spreads into infragranular layer (~22ms). We have to notice that these latencies differences were no significant and that layers II&III and V had limited samples size.

If we compare our layer IV latencies and *RM*s to values recorded in previous work (Quairiaux and al., 2007) we can underline several differences.
Quairiaux recorded a *PW* stimulation latency of 11.4ms ± 3.8 (± *SD*) in layer IV. In our data, *WWD* fitted in this value interval.
Quairiaux calculated a *RM* of 0.97 ± 0.53 (± *SD*) spike per whisker deflection. None of our two medians fits directly into this interval.

If we compare between *Figure 9* and the layer IV *PSTH* of *Figure 15* we see than part of the difference in *RM* with the *WWD* is probably coming from a bigger signal during period T3 (lightly during end of T2). Signal was not returning to a spontaneous level during T3 as Quairiaux showed

it but stayed at an activity of approximately 0.04 spike/deflection (spontaneous activity before stimulation was <0.01 spike/deflection) The peak value during T1 and T2 was also twice more important than in Quairiaux's work. T4 and T5 period were difficult to interpret because of noise. They appeared to respect the behavior of previous findings but seemed also to show, as for T3, a larger signal.

The excessive response magnitude (2-3 times bigger) of the *WWD* in comparison with Quairiaux's work possesses multiple explanations. The differences in excitability can be due to effect of anesthesia, mouse strain and variation in whisker stimulation amplitude.
As seen in previous chapter 6.2, anesthesia levels mainly influence the cortical response. The anesthesia globally increases the amplitude of the response to whisker deflection. In opposition, with the increasing of anesthesia level, cortical activity groups itself into clusters or bursts changing the response to stimulation whether stimulation occurs during burst or not. Maybe the anesthesia level we performed was deeper (or lower) than the one Quairiaux achieved in his previous work, inducing increased response magnitude.
The mouse strain can also explain the discrepancies in magnitude response because of strain-related reaction to anesthesia or to whisker deflection.

The SW response shows shorter latencies in layer V (~30ms) than in layers II&III (~35ms) and layer IV (~51ms) with the *WWD* (the difference was not significant). A hypothesis can be that *SWs* mainly activate the barrel through infragranular connections and that the signal then spread up to the cortical surface. The *SWs* show a fastest response to row whiskers than arc whisker in all 3 layers (the difference was not significant). It corresponds with previous findings that intercolumnar connections are stronger within a row than those in different rows. The *SWs* temporal profile shows predominant response and major contribution to response of row *SWs* stimulation.

11. Conclusion

Our work allows us to compare two different ways of signal discrimination, the *WWD* and the *SSD*. Despite the fact that *SSD* is a powerful method of signal discriminating, we do not succeed to use it for cell signal discriminating and the extracellular recording in *Single Unit Analysis*. The signal we record with this method does not have the profile of cortical cell response in comparison with our *WWD* recordings. In addition, the median values were significantly different in layer IV between *WWD* and *SSD*. This comes probably from the way *SSD* discriminate signal and maybe different templates settings and larger sample size will have permit discrimination of neuronal cells signal with this method.
The *WWD* results in comparison to previous Quariaux's work show some difference but also similarities. The latency we recorded fits with previous work. The *RM* was clearly larger in comparison with previous work and this can be explained by multiple conditions such as a different level of anesthesia or larger amplitude of whisker deflection. The mouse strain we use was also different from Quairiaux's previous study. The *WWD PSTH* profile shows that *RM* is increased during the peak periods but also in the late periods where activity stays at a certain level instead of returning to the spontaneous activity level.
The major limitation in the reliability of our results comes mainly from the small amount of cells recorded.

Conclusion

11. Last words

The aim of the work was to get familiarized with intracortical recordings in an anaesthetized mouse. We had the chance to record the cortical response of 12 mice. The data analysis of these recordings helped me to discover different representations commonly used when we treat with neuronal cell signal. With this, we compared two signal discriminations but unfortunately, the results from the *SSD* method do not fit with previous cortical known response.
This work showed me and made me learn that fundamental science required strictness, patience and a huge amount of imagination. This work gave me the opportunity to familiarize myself with the world and the wonder of electrophysiology.

12. Acknowledgement

First I would like to thanks Egbert Welker for his incommensurable help. Thank you for all these afternoons listening to brain music and other Jazz, as well as for your patience, teaching time, trust and all.
To Roger Dubois who helped me find a way out in front of indecipherable scripts.
To Sonia the energetic part of the lab.
To Christine for the scheme, Ines for saving my mice and Aouatef for the enthusiasm for my work.
To all, thank you for helping me find stuff in this nice and tidy place and for your kindness, it was a real pleasure coming in the lab.
To my dad for lecture and advice.
To all 16 mice that died for my masterwork.
To the coffee machine which will probably die soon.
To the industrial service of the Lausanne City for all energy consume in computer, microscope heating and all.
Thank you all for your support.

References

Armstrong-James M, Fox K. Spatiotemporal diergence and convergence in rat "barrel" cortex. *J Comp Neurol* 263: 265-281, 1987.

Armstrong-James M, Fox K, Das-Gupta A. Flow of excitation within rat barrel cortex on striking a single vibrissa. *J Neurophysiol* 68: 1345-1358, 1992.

Armstrong-James M, George MJ. Influence of anesthesia on spontaneous activity and receptive field size of single units in rat Sm1 neocortex. *Exp Neurol* 99: 369-387, 1988.

Armstrong-James M, Millar JA. Carbon fibre microelectrodes. *J Neurosci Methods* 1: 279-287, 1979.

Bernardo KL, Mc Casland JS, Woolsey TA, Strominger RN. Local intralaminar and interlaminar connections in mouse barrel cortex. *J Comp Neurol* 291: 231-255, 1990.

Diamond ME, Armstrong-James M, Ebner FF. Experience-dependent plasticity in adult-rat barrel cortex. *Proc Natl Acad Sci USA* 90: 2082-2086, 1993.

Douglas RJ, Martin KA. Recurrent neuronal circuits in the neocortex. *Curr Biol* 17: R496-R500, 2007.

Douglas RJ, Martin KA, Witteridge D. A canonical microcircuit for neocortex. *Neural Comput* 1: 480-488, 1989.

Erchova IA, Lebedev MA, Diamond ME. Somatosensory cortical neuronal population activity across states of anaesthesia. *Eur J Neurosci* 15: 744-752, 2002.

Gieselmann MA, Thiele A. Comparison of spatial integration and surround suppression characteristics in spiking activity and the local field potential in macaque V1. *Eur J Neurosci* 28: 447-459, 2008.

Haslinger R, Ulbert I, Moore CI, Brown EN, Devor A. Analysis of LFP Phase Predicts Sensory Response of Barrel Cortex *J Neurophysiol* 96:1658-1663, 2006.

Katzner S, Nauhaus I, Benucci A, Bonin V, Ringach DL, Carandini M. Local origin of field potentials in visual cortex. *Neuron* 61: 35-41, 2009.

Knott GW, Quairiaux C, Genoud C, Welker E. Formation of dendritic spines with GABAergic synapses by whisker stimulation in induced adult mice. *Neuron* 34: 265-273, 2002.

Liu J, Newsome WT. Local field potential in cortical area MT: stimulus tuning and behavioral correlations. *J Neurosci* 26: 7779-7790, 2006.

Mitzdorf U. Current source-density method and application in cat cerebral-cortex: investigation of evoked-potentials and EEG phenomena. *Physiol Rev* 65: 37-100, 1985.

Mountcastle VB. Perceptual Neuroscience: the Cerebral Cortex. *Cambridge, MA: Harvard University Press*, 1998.

Paxinos G. The human nervous system. *Academic Press, San Diego*, pp. 757-813, 2011.

Peters A, Jones EG. Cerebral Cortex. *New York: Plenum* vol. 1, 1984.

Petersen RS, Diamond ME. Spatial-temporal distribution of whisker-evoked activity in rat somatosensory cortex and the coding of stimulus location. *J Neurosci* 20: 6135-6143, 2000.

Petersen C, Grinvald A, Sakmann B. Spatiotemporal dynamics of sensory responses in layer 2/3 of rat barrel cortex measured in vivo by voltage-sensitive dye imaging combined with whole-cell recordings and neuron reconstructions. *J Neurosci* 23: 1298-1309, 2003.

Pikovsky A, Rosenblum M, Kurths J. Synchronization - A Universal Concept in Nonlinear Sciences. *Cambridge, UK: Cambridge*, 2001.

Porter JT, Johnson CK, Agmon A. Diverse types of interneurons generate thalamus-evoked feedforward inhibition in the mouse barrel cortex. *J Neurosci* 21: 2699-2710, 2001.

Quairiaux C. Neurophysiologic and proteomic investigations of experience-dependent plasticity in the somatosensory cortex of the adult mouse following chronic whisker stimulation, 2005.

Quairiaux C, Armstrong-James M, Welker E. Modified sensory processing in the barrel cortex of the adult mouse after chronic whisker stimulation. *J Neurophysiol* 97: 2130-2147, 2007.

Rocamora N, Welker E, Pascual M, Soriano E. Upregulation of BDNF mRNA expression in the barrel cortex of adult mice after sensory stimulation. *J Neurosci* 16: 4411-4419, 1996.

Rohkamm R. Atlas de poche de Neurologie. *Médecine-Science – Flammarion*, 2005.

Simons DJ, Carvell GE, Hershey AE, Bryant DP. Responses of barrel cortex neurons in awake rats and effects of urethane anesthesia. *Exp Brain Res* 91: 259-272, 1992.

Smith TG Jr, Lecar H, Redman SJ, Gage PW. Voltage and patch clamping with microelectrodes. *American* -0.5 *physiological society*, 1985.

Spike2 for Windows, version 7. User manual. *Cambridge Electronic Design , 2009.*

Steriade M, Nunez A, Amzica F. A novel slow (< 1 Hz) oscillation of neocortical neurons in vivo: depolarizing and hyperpolarizing components. *J Neurosci* 13: 3252-3265, 1993.

Temereanca S and Simons DJ. Local field potentials and the encoding of whisker deflections by population firing synchrony in thalamic barreloids. *J Neurophysiol* 89: 2137-2145, 2003.

Valverde F. Intrinsic neocortical organization: some comparative aspects. *Neuroscience* 18: 1-23, 1986.

Woolsey TA, Van der Loos H. The structural organization of layer IV in the somatosensory region (SI) of mouse cerebral cortex. *Brain Res* 17: 202-242, 1970.

Welker E, Armstrong-James M, Van der Loos H, Kraftsik R. The mode of activation of a barrel column: response properties of single units in the somatosensory cortex of the mouse upon whisker deflection. *Eur J Neurosci* 5: 691-712, 1993.

Welker E, Rao SB, Dörfl J, Melzer P, Van der Loos H. Plasticity in the barrel cortex of the adult mouse: effects of chronic stimulation upon deoxyglucose uptake in the behaving animal. *J Neurosci* 12: 153-170, 1992.

Welker E, Soriano E, Dörfl J, Van der Loos H. Plasticity in the barrel cortex of the adult mouse: transient increase of GAD-immunoreactivity following sensory stimulation. *Exp Brain Res* 78: 659-664, 1989.

Welker E, Armstrong-James M, Van der Loos H, Kraftsik R. The mode of activation of a barrel column: response properties of single units in the somatosensory cortex of the mouse upon whisker deflection. *Eur J Neurosci* 5: 691-712, 1993.

Appendix. Scheme representing the different modules arrangement required to proceed signal coming from the cortical microelectrode.